The Iranian Journal of Mechanical Engineering Transactions of ISME
Journal homepage: https://jmee.isme.ir/
Vol. 25, No. 1, 2024, pp. 130-142

Research Paper

DOI: https://doi.org/10.30506/jmee.2024.2014715.1326

A Simulation Study on Ionic Current in Cylindrical Hydrophobic Nanopores

Ali Shafiei Souderjani[1]
M.Sc.

Mohammad Hassan Saidi[2]
Professor

The ionic current and electroosmotic flow (EOF) are studied in hydrophobic nanopores numerically. The Poisson, Stokes, and Nernst-Planck equations were solved simultaneously by finite element method. For the characterization of hydrophobic nanopores, the Navier-slip boundary condition was replaced the no-slip boundary condition on the surface of the nanopore, and a wide range of slip lengths is used in order to cover all the possible hydrophobic conditions. The effect of hydrophobicity on different ionic current mechanisms is investigated. Also, the effects of voltage difference, electrolyte concentration, and radius of nanopore on the ionic current in hydrophobic nanopores are studied. The results show that nanopore hydrophobicity affects the convective and electrophoretic ionic current significantly. Due to the EOF enhancement by increasing the nanopore's slip length, the convective ionic current signifies, and the electrophoretic ionic current dwindles.

Keywords: Nanopore, Hydrophobicity, Ionic current, Eletroosmotic flow, Creeping flow

1 Introduction

By the development of the nano-fabrication tools, the nano sensors and devices are used in biology fields for the detection of bio-particles and DNA sequencing, massively [1, 6]. Nanopores are categorized into two groups: biological and solid-state nanopores [7]. Solid-state nanopores could be manufactured in different sizes, and the surface properties can be modified with the fabrication processes [8-14]. As the ratio of the surface to volume in the nano scale devices is very high, surface properties play key roles in the design of such systems.

[1]M.Sc., Department of Mechanical Engineering, Sharif University of Technology, Tehran, Iran, ali.shafie.s20@gmail.com
[2]Corresponding Author, Professor, Department of Mechanical Engineering, Sharif University of Technology, Tehran, Iran, saman@sharif.edu

Received: 2023/10/30, Revised: 2024/01/16, Accepted: 2024/04/14

In some nanopores and nanotubes like carbon nanotubes, and boron nitride nanotubes, non-wettability characteristics have been seen [15-20].
Hydrophobicity of nanopore characterizes with slip length of walls which is an extrapolate distance into the wall, and the tangential velocity on the surface of walls has a direct relation with the slip length and the shear stress.
Even a small slip length of nanopore or particles could completely change the condition for the motion of ions and particle in the nanopore. Shafiei Souderjani et al. [21] have shown that when the slip length is non-zero on the surface of particles, the velocity of particle due to the reduction in the friction force increases dramatically. Also, when the particle goes through the nanopore, the resistance of nanopore enhances due to the blocking effect of particle. Therefore, the resistive pulse sensing could be used for the detection of particles. Shafiei Souderjani et al. [21] have investigated that hydrophobicity and surface property also change the resistive pulse sensing magnificently. So, it is necessary to examine the effect of hydrophobicity of nanopores on the ionic current.
When the nanopore's wall which has surface charge density is in contact with electrolyte, a thin layer of ions with opposite sign generates near the wall. By exerting an electric field, a volume electric force creates electroosmotic stream in the nanopore. Hydrophobicity of wall has a significant effect on the strength of this EOF stream. Researches have shown that electrophoretic velocity increases by a factor of $(1 + \lambda_w \kappa)$ which λ_w is the slip length of wall and κ is the reverse of electric double layer size [22, 23]. In usual biological studies, the size of electric double layer is in order of nanometer. So, even in the small amount of slip length, electroosmotic velocity enhances significantly which affects the ionic current in the nanopore. Recently, Pandey et al. [24] investigated the effect of hydrophobicity on the ionic current. But they considered the size of ions. In this study, since the surface charge density of walls in the hydrophobic nanopores is small, we consider the ions like points.
Three different mechanisms contribute in the motion of ions in nanopore. The first mechanism is due to the electrolyte concentration effect on the two sides of nanopore. This effect could be negligible when the electrolyte concentration is equal in the reservoirs. The second mechanism creates because of the flow motion in the nanopore. Electroosmotic flow moves ions through the nanopore. The direction motion of EOF in the nanopore depends on the sign of nanopore surface charge density. The last ion movement mechanism in the nanopore is due to the effect of electric field on the charged ions. Negative ions and positive ions tend to move toward anode and cathode, respectively. In the present study, at first, the effect of hydrophobicity on the motion of ions due to the three different mechanisms is examined. In continue, the effect of electrolyte concentration, electric field, and size of nanopore in the motion ions in hydrophobic nanopore is investigated.

2 Governing equations and boundary conditions

In order to model the motion of ions in the hydrophobic nanopore, the continuum approach is chosen. Since the Knudsen number which is the ratio of mean free pass to the minimum feature of physical domain, is lower than 0.001, the assumption of continuum model is valid [25,26]. In fact, when the fluid is water, for nanopores with radius larger than 4 nm, the continuum approach could be used. For the simulation of ion transport, the Poisson, Stokes and Nernst-Planck equations must be solved simultaneously. In Figure (1), the domain of solution is demonstrated. Since the domain of solution is 2D axis symmetric, a cylindrical coordinate (r, z) is placed in the center of nanopore. The hydrophobic nanopore is connected to two reservoirs. The equation (1) is the Poisson equation which represents the electric field distribution. To generate an electric field, a potential difference must be applied to the two sides of the reservoirs. The potential of AB segment is set to the zero and a positive potential is applied to the HG border. The constant -0.01 $\frac{\mathrm{C}}{\mathrm{m}^2}$ charge surface boundary condition is used for the surface of nanopore. The borders of reservoirs have zero charge density and the symmetry boundary condition is assigned to the HA segment.

$$-\nabla(\varepsilon_0\varepsilon_r\nabla\varphi) = F\sum_i c_i z_i \quad (1)$$

$$\vec{E} = -\nabla\varphi \quad (2)$$

$$\varphi_{AB} = 0\ mV \quad (3)$$

$$\varphi_{GH} = V\ mV \quad (4)$$

$$n.(-\varepsilon_0\varepsilon_r\nabla\varphi) = \sigma_w \quad \text{on CD، DE، and EF} \quad (5)$$

$$n.(-\varepsilon_0\varepsilon_r\nabla\varphi) = 0 \quad \text{on BC، FG، and HA} \quad (6)$$

In the above equations, φ represents potential, $\varepsilon_0 = 8.85 \times 10^{-12}\frac{F}{m}$ and $\varepsilon_r = 80$ are absolute and relative permittivity, $F = 96485.3\ \frac{C}{m}$ is faraday constant, c_i and $z_i = \mp 1$ are concentration and valence each ion respectively, $\vec{E}$ represents electric field and σ_w is the surface charge density of nanopore. For finding the fluid velocity in the domain of solution, the continuum and Navier-Stokes equations must be solved. Since the Reynolds number is much smaller in nano scale, the inertial term in the Navier-Stokes equation is neglected. Also, an additional term for representing electric force is added to the Stokes equation.

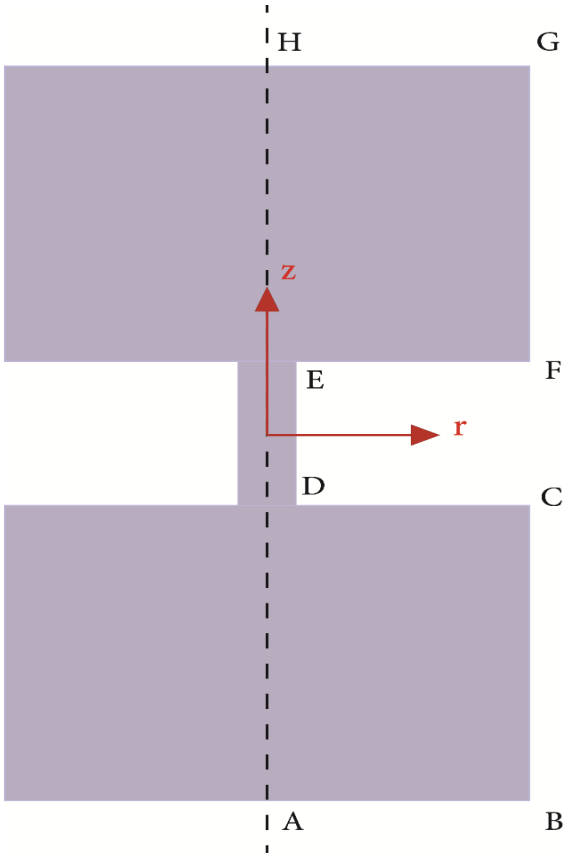

Figure 1 The numerical domain including the hydrophobic nanopore and two reservoirs

As mentioned before, the Navier-slip boundary condition replaces no-Slip boundary condition. In figure (1), FE, ED, and DC are nanopore's walls. The no-slip boundary condition is applied on the GF and CB borders. Since there is no external hydrodynamic pressure, the pressure of AB and HG boundaries is set to zero. Also, symmetry boundary condition is used for AH border.

$$\nabla . u = 0 \tag{7}$$

$$-\nabla P + \mu \nabla^2 u - \rho_e \nabla \varphi = 0 \tag{8}$$

$$u = 0 \quad on\ AB\ and\ HG \tag{9}$$

$$p = 0 \quad on\ GF\ and\ CB \tag{10}$$

$$u^{||} = \lambda_w \frac{\tau}{\mu}, u^{\perp} = 0 \quad on\ CD\,.\ DE\,.\ and\ EF \tag{11}$$

In above equations, u and P are velocity and pressure in the domain, respectively. $\mu = 0.001$ Pa. s is dynamic viscosity, ρ_e is the net charge density of electrolyte and is equal to $F \sum_i c_i z_i$. $u^{||}$ and $u^{\perp}$ are the slip velocity and the normal velocity. Also τ and λ_w represent the shear stress and the slip length of nanopore's wall, respectively.
The distribution of ions characterizes with Nernst-Planck equation. N_i is the total anion and cation fluxes. D_i, $R = 8.3185\ \frac{\text{J}}{\text{mol.K}}$, and $T = 298$ K are diffusion coefficient of anions and cations, universal gas constant, and temperature, respectively. The proper boundary conditions for Nernst-Plank equation are expressed in the following:

$$\nabla . \overrightarrow{N_\iota} = 0 \tag{12}$$

$$\overrightarrow{N_\iota} = u c_i - D_i \nabla c_i - z_i \frac{D_i}{RT} F c_i \nabla \varphi \tag{13}$$

$$\overrightarrow{N_\iota} = 0 \quad on\ BC\,.\ CD\,.\ DE\,.\ EF\,.\ and\ FG \tag{14}$$

$$c_i = c_0 \quad on\ AB\ and\ GH \tag{15}$$

3 Numerical model and validation

The nanopores with radius a and height h, is filled with KCL. The electrolyte is symmetric. The diffusion coefficients of Potassium and chloride are 1.97×10^{-9} and 2.03×10^{-9}. To calculate the ionic current and EOF in the domain of solution, above equations must be solved simultaneously. A finite element package is used to solve the equations. A non-structured mesh with finer elements near the walls is used and for the case of $c_0 = 100\ mM$, and $\varphi_{GH} = 0.5\ V$, the mesh independency is checked. The mesh independency diagram is demonstrated in Figure (2). Since the variation of parameters is not high in the reservoirs, a coarser mesh structure is used to keep the cost of calculation low.

After solving equations, for calculation of ionic current must be calculated far away from the nanopore's wall. If the ionic current measures in the nanopore, since the presence of electric double layer, the results will not be valid. For the validation of numerical method, the results of experimental research of Qiu et al. [27] is used. Qiu et al. [27] calculated the ionic current in a conical nanopore with high of 11 micrometers, the lower radius of 355 nanometers, and upper radius of 1100 nanometers. The nanopore filled with 100 mM KCl electrolyte. A wide range of voltages is applied in the two sides of nanopore, and ionic current is measured. As shown in Figure (3), the numerical results are in a good agreement with experimental results.

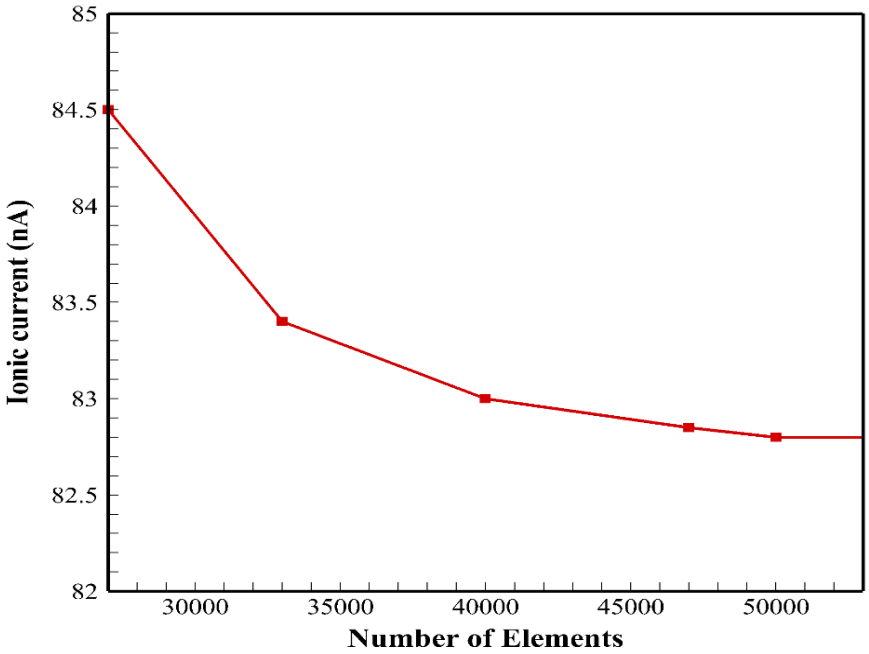

Figure 2 The ionic current versus number of elements

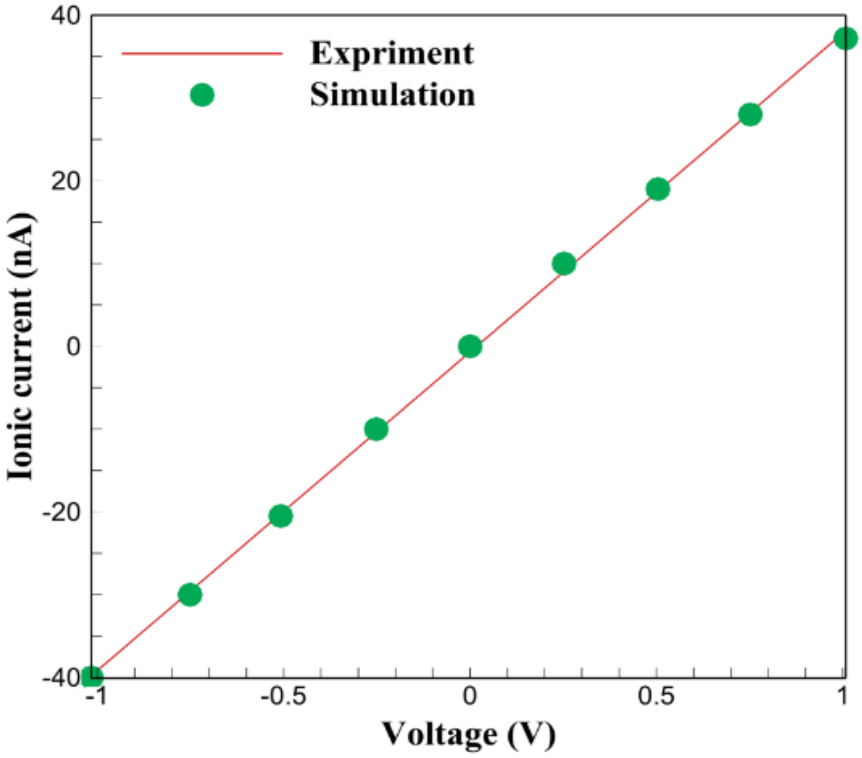

Figure 3 Validation of numerical model with exprimental research of Qiu et al. [27]

4 Results

Three mechanisms contribute in the ionic current in a nanopore: convection, diffusion, and electrophoretic motion of ions. In this section, the effect of wall's hydrophobicity on each mechanism is investigated. To study the effect of hydrophobicity, the electrolyte concentration, and voltage, a nanopore with radius of 250 nanometer and height of 500 nanometer is used.

4.1 The effect of hydrophobicity on the ion transport mechanisms

As mentioned before, the hydrophobicity of the nanopore's wall increases the EOF velocity. To study the effect of hydrophobicity on the ion transport mechanisms, the electrolyte concentration is assumed to be 100 mM, and the voltage difference is equal to 0.5 V. According to the following equation, when the electrolyte concentration is 100 mM, the thickness of electric double layer (EDL) is approximately equal to 1 nm. Thus, for the conditions that the slip is greater than 1nm, the EOF enhances with the growth of slip length. In Figure (4), the EOF is plotted against the slip length. As illustrated, the difference between the EOF in hydrophobic and hydrophilic nanopores could be distinguished completely. In fact, the velocity of fluid in hydrophobic nanopores is much more than hydrophilic nanopores. This enhancement in the EOF could be beneficial in some cases. For instance, nanopores could be used as filters for water purification, and hydrophobic nanopores increase the amount of water purification compared to the hydrophilic nanopores.

$$\kappa^{-1} = \left[\frac{2F^2 c_0}{\varepsilon_0 \varepsilon_r RT}\right]^{-\frac{1}{2}} \tag{16}$$

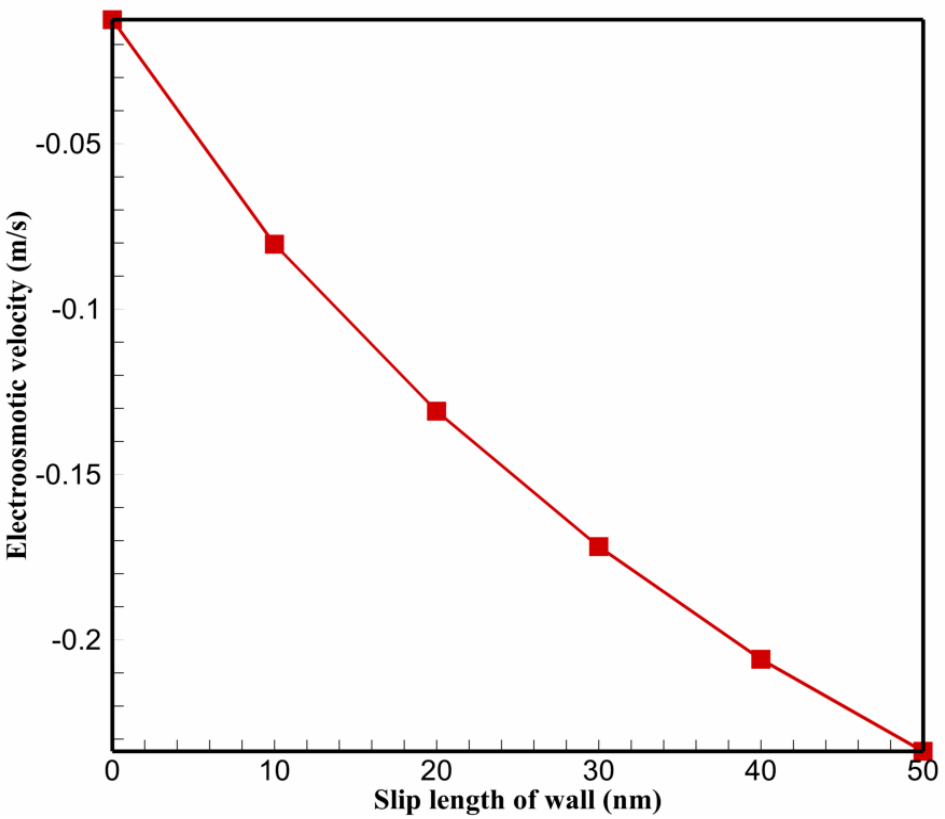

Figure 4 EOF velocity versus slip length. The electrolyte concentration is equal to 100 mM, and the potential difference is set to 0.5 V.

In Figure (5), the total ionic current and three different ion current mechanisms versus slip length are demonstrated. Due to the EOF velocity enhancement, convective ionic by slip length increases. In fact, the convective ionic current is due to the fluid velocity. Since the EOF velocity experiences a large growth, the convective mechanism is also enhanced extensively. In contrast to the convective part, by increasing the slip length, the electrophoretic ionic current dwindles. In addition, the amount of diffuse ion current is so small compared to the two other ionic currents and can be neglected. Finally, as illustrated in Figure (5), the total ionic current increases with slip length. This enhancement in the total ionic current could help to generate a resistive pulse with a higher domain. Therefore, the ratio of ionic current to the noise will be greater, and the resistive pulse with a higher resolution will be used for the characterization of particles and DNA in the nanopore.

4.2. The effect of electrolyte concentration

The concentration of electrolyte determines the size of the electric double layer. By increasing the electrolyte concentration, a thinner electric double layer forms around the charged walls. The size Debye length also affects the EOF velocity and finally changes the ionic current. In Figure (6), the amount of ionic current versus the slip length for various range electrolyte concentrations is plotted. When the electrolyte concentration in the reservoirs enhances, the number of ions that crosses the nanopore growths. But the slip length does not have the same effect on the increase of ionic current for all electrolyte concentrations. As shown in Figure (6), the growth of ionic current with slip length is more in the electrolytes with higher concentration. As mentioned, the ratio of slip length and EDL size determines the amount of increase in the EOF velocity. As a result, when the electrolyte concentration is high, this ratio will be much more, and the EOF affects the ionic current.

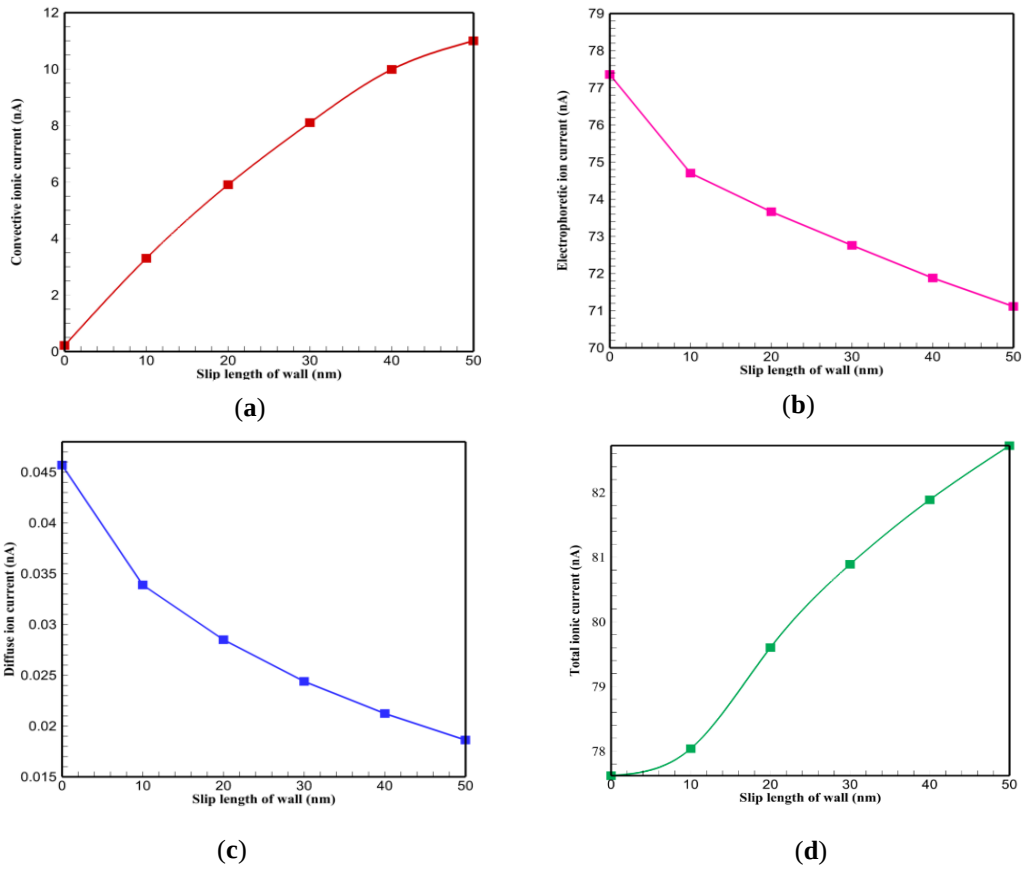

Figure 5 a) Convective ionic current versus slip length, b) Electrophoretic ionic current versus slip length, c) Diffuse ion current versus slip length, and d) Total ionic cureent versus slip length.

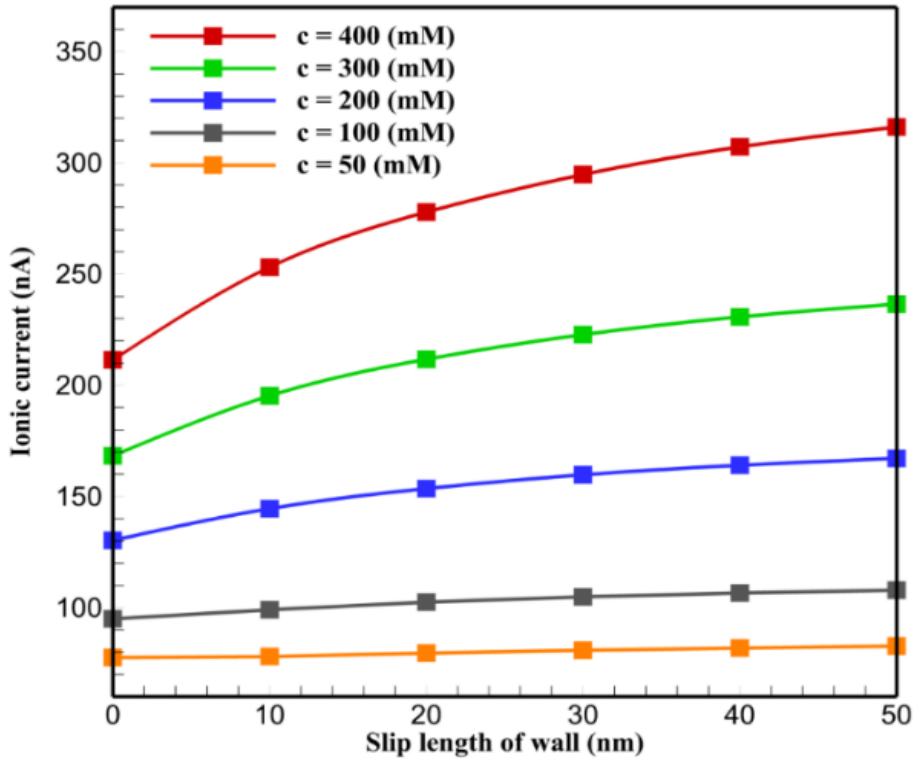

Figure 6 Ionic current versus slip length of wall for different electrolyte concentrations

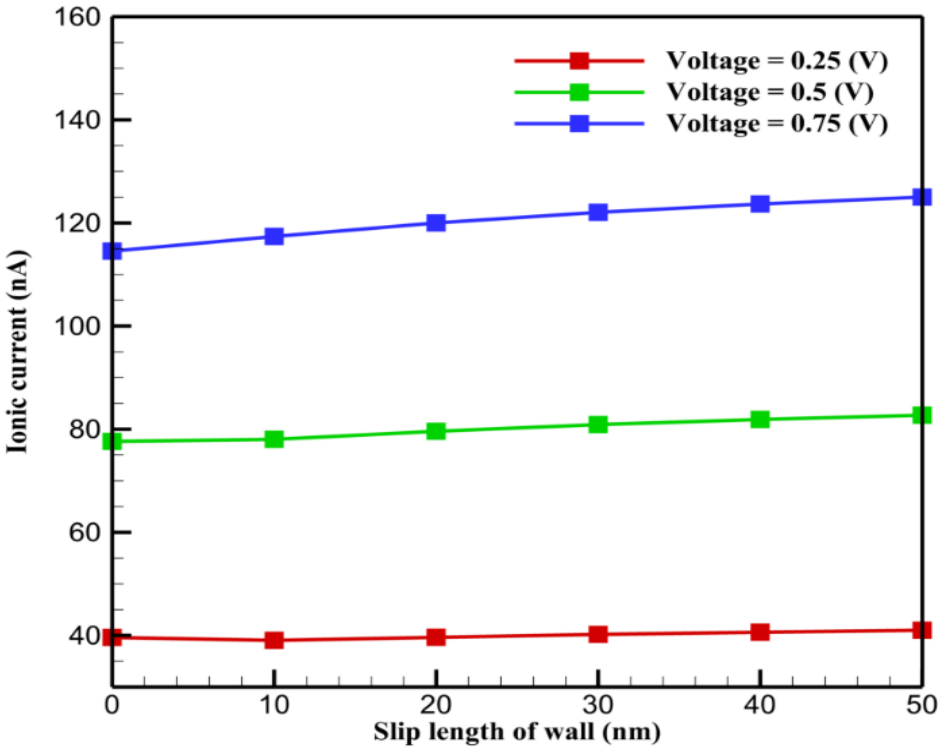

Figure 7 Ionic current versus slip length of wall for different voltages

4.3 The effect of potential difference

When a potential difference between two sides of the nanopore is exerted, the electric force moves the ions toward the electrodes with the opposite sign. The strength of electric force depends on the potential difference.

In Figure (7), the ionic current against the slip length is plotted for three voltage differences. By increasing the voltage, the ionic current enhances due to the more powerful electric force. But, the hydrophobicity of the nanopore's wall almost has the same effect on the ionic current for different potential differences. The increase in the potential difference also could enhance the velocity of particles in the nanopore due to the effect of electric force. Although, the more powerful potential difference creates stronger ionic current in nanopore, it can cause problems for the detection of particle.
In fact, the particle moves faster through the nanopore, and the resistive pulse width could not be distinguishable for particles with different properties. As a results, it is necessary to choose proper potential difference for the detection of particles in the nanopores. In the case of hydrophobic nanopore, it shows that design of potential difference should occur based on velocity of particle instead of ionic current in the nanopore.

4.4 The effect of nanopore radius

In the previous sections, the radius of nanopore was 250 nm. In this section, the effect of radius of nanopore on the ionic current is investigated. The nanopore could be considered as a wire which has resistive for crossing of the electric current. Therefore, when the radius of nanopore changes, the resistive of nanopore for the crossing of ions also alters. In Figure (8), the ionic current is plotted versus slip length for three different nanopore radius. As expected, the ionic current for the nanopore with radius of 350 nm is higher than two other cases. However, by increasing the slip length, the ionic current trend is the same for three different radii, and the results show that hydrophobic nanopore are not sensitive to the radius of nanopore.

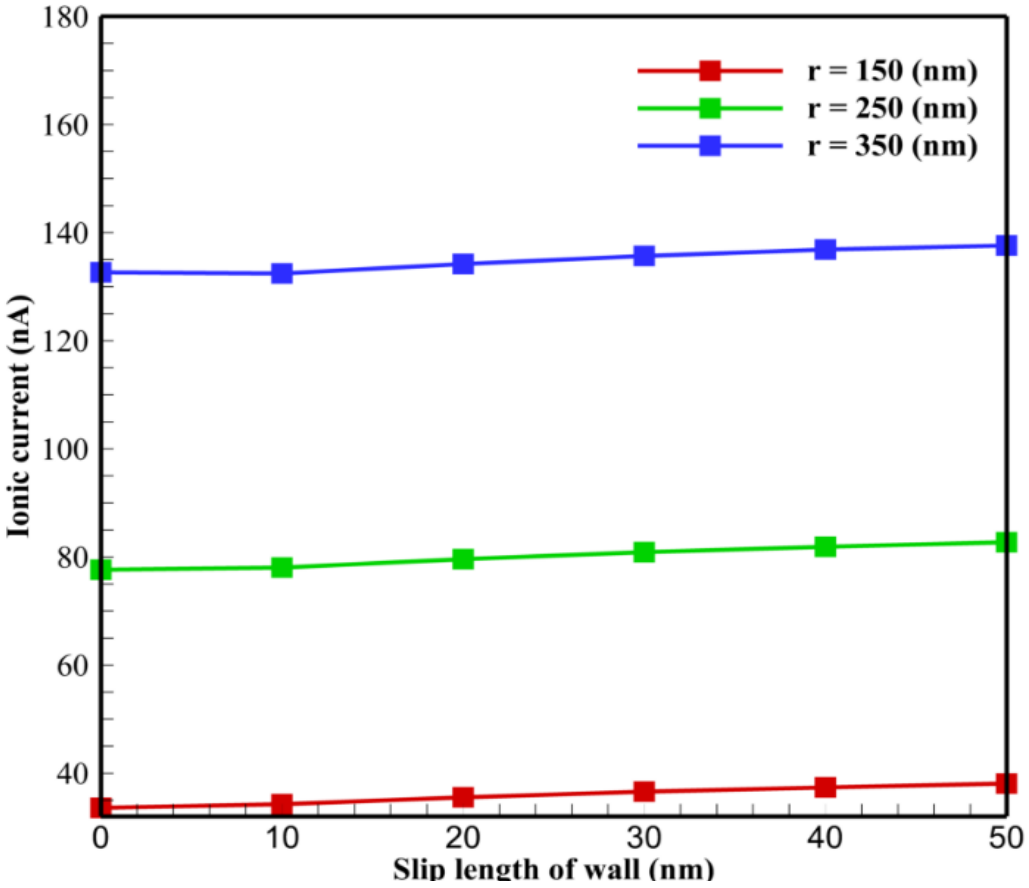

Figure 8 Ionic current versus slip length of wall for nanopores with different radius

5 Conclusions

This study investigates the effect of the nanopore wall hydrophobicity on the ionic current. The Poisson, Navier-Stokes, and Nernst-Planck Equations with a finite element package are solved simultaneously to find the ionic current and EOF velocity. For the characterization of hydrophobicity, the Navier slip boundary condition replaces the no-slip boundary condition. In addition, a term for the electric force is added to the Stokes equation. To validate the scheme of the solution, the results of an experimental study are compared with a numerical solution that had a good agreement. The results show that by increasing the slip length, convective and total ionic currents increase, but the electrophoretic ionic current decreases; also, by enhancement of the electrolyte concentration, the effect of hydrophobicity on ionic current growths. But, the slip length has the same effect for different potential differences and nanopore's radius.

References

[1] I. M. Derrington, T.Z. Butler, M.D. Collins, E. Manrao, M. Pavlenok, M. Niederweis, and J.H. Gundlach, "Nanopore DNA Sequencing with MspA," *Proceedings of the National Academy of Sciences,* Vol. 107, No. 37, pp. 16060-16065, 2010, Doi: https://doi.org/10.1073/pnas.1001831107.

[2] J. Clarke, H.-C. Wu, L. Jayasinghe, A. Patel, S. Reid, and H. Bayley, "Continuous Base Identification for Single-molecule Nanopore DNA Sequencing," *Nature Nanotechnology*, Vol. 4, No. 4, pp. 265-270, 2009, Doi: https://doi.org/10.1038/nnano.2009.12.

[3] G. F. Schneider and C. Dekker, "DNA Sequencing with Nanopores," *Nature Biotechnology*, Vol. 30, No. 4, pp. 326-328, 2012, Doi: https://doi.org/10.1038/nbt.2181.

[4] T. Z. Butler, M. Pavlenok, I. M. Derrington, M. Niederweis, and J. H. Gundlach, "Single-molecule DNA Detection with an Engineered MspA Protein Nanopore," *Proceedings of the National Academy of Sciences*, Vol. 105, No. 52, pp. 20647-20652, 2008, Doi: https://doi.org/10.1073/pnas.0807514106.

[5] A. Fanget, F. Traversi, S. Khlybov, P. Granjon, A. Magrez, L. Forró, and A. Radenovic, "Nanopore Integrated Nanogaps for DNA Detection," *Nano Letters,* Vol. 14, No. 1, pp. 244-249, 2014, Doi: https://doi.org/10.1021/nl403849g.

[6] A. Barati Farimani, P. Dibaeinia, and N. R. Aluru, "DNA Origami–graphene Hybrid Nanopore for DNA Detection," *ACS Applied Materials & Interfaces,* Vol. 9, No. 1, pp. 92-100, 2017, Doi: https://doi.org/10.1021/acsami.6b11001.

[7] Z. Liu, X. Shi, and H. Wu, "Coarse-grained Molecular Dynamics Study of Wettability Influence on Protein Translocation Through Solid Nanopores," *Nanotechnology,* Vol. 30, No. 16, p. 165701, 2019, Doi: 10.1088/1361-6528/aafdd7.

[8] M. Waugh, K. Briggs, D. Gunn, M. Gibeault, S. King, Q. Ingram, A.M. Jimenez, S. Berryman, D. Lomovtsev, L. Andrzejewski, and V. Tabard-Cossa, "Solid-state Nanopore Fabrication by Automated Controlled Breakdown," *Nature Protocols*, Vol. 15, No. 1, pp. 122-143, 2020, Doi: https://doi.org/10.1038/s41596-019-0255-2.

[9] A. Storm, J. Chen, X. Ling, H. Zandbergen, and C. Dekker, "Fabrication of Solid-state Nanopores with Single-nanometre Precision," *Nature Materials*, Vol. 2, No. 8, pp. 537-540, 2003, Doi: https://doi.org/10.1038/nmat941.

[10] Y. Goto, I. Yanagi, K. Matsui, T. Yokoi, and K.-i. Takeda, "Integrated Solid-state Nanopore Platform for Nanopore Fabrication Via Dielectric Breakdown, DNA-speed Deceleration and Noise Reduction," *Scientific Reports*, Vol. 6, No. 1, p. 31324, 2016, Doi: https://doi.org/10.1038/srep31324.

[11] R. Dela Torre, J. Larkin, A. Singer, and A. Meller, "Fabrication and Characterization of Solid-state Nanopore Arrays for High-throughput DNA Sequencing," *Nanotechnology*, Vol. 23, No. 38, p. 385308, 2012, Doi: 10.1088/0957-4484/23/38/385308.

[12] M. Wanunu and A. Meller, "Chemically Modified Solid-state Nanopores," *Nano Letters*, Vol. 7, No. 6, pp. 1580-1585, 2007, Doi: https://doi.org/10.1021/nl070462b.

[13] J. Kudr, J. Kudr, S. Skalickova, L. Nejdl, A. Moulick, B. Ruttkay–Nedecky, V. Adam, and R. Kizek "Fabrication of Solid-state Nanopores and Its Perspectives," *Electrophoresis*, Vol. 36, No. 19, pp. 2367-2379, 2015, Doi: https://doi.org/10.1002/elps.201400612.

[14] K. Briggs, H. Kwok, and V. Tabard-Cossa, "Automated Fabrication of 2-nm Solid-State Nanopores for Nucleic Acid Analysis," *Small*, Vol. 10, No. 10, pp. 2077-2086, 2014, Doi: https://doi.org/10.1002/smll.201303602.

[15] J.-Y. Jung, P. Joshi, L. Petrossian, T. J. Thornton, and J. D. Posner, "Electromigration Current Rectification in a Cylindrical Nanopore Due to Asymmetric Concentration Polarization," *Analytical Chemistry*, Vol. 81, No. 8, pp. 3128-3133, 2009, Doi: https://doi.org/10.1021/ac900318j.

[16] S. Balme, S. Balme, F. Picaud, M. Manghi, J. Palmeri, M. Bechelany, S. Cabello-Aguilar, A. Abou-Chaaya, P. Miele, E. Balanzat, and J. M. Janot, "Ionic Transport Through Sub-10 nm Diameter Hydrophobic High-aspect Ratio Nanopores: Experiment, Theory and Simulation," *Scientific Reports*, Vol. 5, No. 1, p. 10135, 2015, Doi: https://doi.org/10.1038/srep10135.

[17] M. R. Powell, L. Cleary, M. Davenport, K. J. Shea, and Z. S. Siwy, "Electric-field-induced Wetting and Dewetting in Single Hydrophobic Nanopores," *Nature Nanotechnology*, Vol. 6, No. 12, pp. 798-802, 2011, Doi: https://doi.org/10.1038/nnano.2011.189.

[18] J. Polster, E. T. Acar, T. A. Pham, and Z. S. Siwy, "Gating of Hydrophobic Nanopores with Large Anions," *Biophysical Journal*, Vol. 118, No. 3, pp. 158a-159a, 2020, Doi: https://doi.org/10.1021/acsnano.9b09777.

[19] T. Haynes, I. P. Smith, E. J. Wallace, J. L. Trick, M. S. Sansom, and S. Khalid, "Electric-field-driven Translocation of ssDNA Through Hydrophobic Nanopores," *ACS Nano*, Vol. 12, No. 8, pp. 8208-8213, 2018, Doi: https://doi.org/10.1021/acsnano.8b03365.

[20] A. Asatekin and K. K. Gleason, "Polymeric Nanopore Membranes for Hydrophobicity-based Separations by Conformal Initiated Chemical Vapor Deposition," *Nano Letters*, Vol. 11, No. 2, pp. 677-686, 2011, Doi: https://doi.org/10.1021/nl103799d.

[21] A. Shafiei Souderjani, M. Bakouei, M. H. Saidi, and M. Taghipoor, "Electrophoretic motion of hydrophobic spherical particles in nanopore: Characteristics, Separation, and Resistive Pulse Sensing," *Physics of Fluids*, Vol. 35, No. 2, 2023, Doi: https://doi.org/10.1063/5.0136454.

[22] A. V. Belyaev and O. I. Vinogradova, "Electro-osmosis on Anisotropic Superhydrophobic Surfaces," *Physical Review Letters*, Vol. 107, No. 9, p. 098301, 2011, Doi: https://doi.org/10.1103/PhysRevLett.107.098301.

[23] M. Manghi, J. Palmeri, K. Yazda, F. Henn, and V. Jourdain, "Role of Charge Regulation and Flow Slip in the Ionic Conductance of Nanopores: An Analytical Approach," *Physical Review E*, Vol. 98, No. 1, p. 012605, 2018, Doi: https://doi.org/10.1103/PhysRevE.98.012605.

[24] D. Pandey and S. Bhattacharyya, "Impact of Surface Hydrophobicity and Ion Steric Effects on the Electroosmotic Flow and Ion Selectivity of a Conical Nanopore," *Applied Mathematical Modelling*, Vol. 94, pp. 721-736, 2021, Doi: https://doi.org/10.1016/j.apm.2021.01.035.

[25] A. Velasco, S. Friedman, M. Pevarnik, Z. Siwy, and P. Taborek, "Pressure-driven Flow Through a Single Nanopore," *Physical Review E*, Vol. 86, No. 2, p. 025302, 2012, Doi: https://doi.org/10.1103/PhysRevE.86.025302.

[26] S. Movahed and D. Li, "Electrokinetic Motion of a Rectangular Nanoparticle in a Nanochannel," *Journal of Nanoparticle Research*, Vol. 14, pp. 1-15, 2012, Doi: https://doi.org/10.1007/s11051-012-1032-0.

[27] Y. Qiu, I. Vlassiouk, Y. Chen, and Z. S. Siwy, "Direction Dependence of Resistive-pulse Amplitude in Conically Shaped Mesopores," *Analytical Chemistry*, Vol. 88, No. 9, pp. 4917-4925, 2016, Doi: https://doi.org/10.1021/acs.analchem.6b00796.

Nomenclature

English symbols

c_i Electrolyte concentration
D_i Diffusion coefficient
$\vec{E}$ Electric field
F Faraday constant
$\overrightarrow{N_i}$ Total ion flux
p Pressure
R Universal gas constant
T Temperature
u Velocity field
$u^{\perp}$ Normal velocity
$u^{||}$ Tangential velocity
V Potential difference
z_i Valence of ions
ε_0 Absolute permittivity
ε_r Relative permittivity
κ Reverse of Deby length

λ_w Slip length
μ Dynamic viscosity
ρ_e Net charge density of electrolyte
τ Shear stress
σ_w Surface charge density of wall
φ Electric potential